



Patterns in forage fish mercury concentrations across Northeast US estuaries

Kate L. Buckman^{a,*}, Robert P. Mason^b, Emily Seelen^{b,1}, Vivien F. Taylor^c,
Prentiss H. Balcom^{b,2}, Jonathan Chipman^d, Celia Y. Chen^a

^a Department of Biological Sciences, Dartmouth College, Hanover, NH, 03755, USA

^b Department of Marine Sciences, University of Connecticut, Groton, CT, 06340, USA

^c Department of Earth Sciences, Dartmouth College, Hanover, NH, 03755, USA

^d Department of Geography, Dartmouth College, Hanover, NH, 03755, USA

ARTICLE INFO

Keywords:

Methylmercury
Landscape
Biogeochemistry
Fish
Estuary

ABSTRACT

Biogeochemical conditions and landscape can have strong influences on mercury bioaccumulation in fish, but these effects across regional scales and between sites with and without point sources of contamination are not well understood. Normal means clustering, a type of unsupervised machine learning, was used to analyze relationships between forage fish (*Fundulus heteroclitus* and *Menidia menidia*) mercury (Hg) concentrations and sediment and water column Hg and methylmercury (MeHg) concentrations, ancillary variables, and land classifications within the sub-watershed. The analysis utilized data from 38 sites in 8 estuarine systems in the Northeast US, collected over five years. A large range of mercury concentrations and land use proportions were observed across sites. The cluster correlations indicated that for *Fundulus*, benthic and pelagic Hg and MeHg concentrations were most related to tissue concentrations, while *Menidia* Hg was most related to water column MeHg, reflecting differing feeding modes between the species. For both species, dissolved MeHg was most related to tissue concentrations, with sediment Hg concentrations influential at contaminated sites. The models considering only uncontaminated sites showed reduced influence of bulk sediment MeHg for both species, but *Fundulus* retained sediment drivers at some sites, with dissolved MeHg still highly correlated for both. Dissolved organic carbon (DOC), chlorophyll, land use, and other ancillary variables were of lesser importance in driving bioaccumulation, though DOC was strongly related within some clusters, likely in relation to dissolved Hg. Land use, though not of primary importance, showed relationships opposite to those observed in freshwater, with development positively correlated and forests and agriculture negatively correlated with tissue concentrations across clusters and species. Clusters were composed of sites from geographically distinct systems, indicating the greater importance of small scale drivers of MeHg formation and uptake into the food web over system or region-wide influences.

1. Introduction

Mercury (Hg), a ubiquitous contaminant, can be transformed to a more bioavailable organic form, methylmercury (MeHg), which is known to bioaccumulate in aquatic organisms and biomagnify in food webs, leading to deleterious effects in resident fauna and organisms that consume them (Eagles-Smith et al., 2018; Sunderland, 2007). Fish consumption advisories for Hg exist in all 50 states to protect human

health, for both fresh and coastal waters. Understanding drivers of Hg bioaccumulation into aquatic food webs is important to predict where fish tissues might exceed environmental and human health criterion as well as to mitigate exposure in contaminated sites without the need for extensive measurements. Estuaries are important repositories for aquatic contaminants like Hg, receiving both watershed and atmospheric inputs (Amos et al., 2014; Chen et al., 2008). They are efficient methylating environments, facilitating the transformation of inorganic

* Corresponding author.

E-mail address: Kate.L.Buckman@dartmouth.edu (K.L. Buckman).

¹ Department of Earth Sciences, University of Southern California, Los Angeles CA 90089.

² John A. Paulson School of Engineering and Applied Sciences, Harvard University, Cambridge MA 02138.

Hg to MeHg (Schartup et al., 2013, 2014) and its subsequent entry into the food web (Chen et al., 2014). Estuaries are also critical habitat for commercially important fish and invertebrate species. They are important environments in mediating mercury cycling, but are chemically and biologically complex on both spatial and temporal scales, complicating understanding of Hg fate in these systems. Combined analysis of multiple diverse estuaries allows for evaluation of the presence (or absence) of consistent general drivers of MeHg bioaccumulation in these important ecosystems.

Previous meta-analyses in upland freshwater ecosystems, particularly, lakes, streams, and rivers, have indicated a wide array of factors influencing Hg dynamics and fate (Chen et al., 2005; Eagles-Smith et al., 2016a; Lavoie et al., 2019; Lavoie et al., 2013; Riva-Murray et al., 2020; Wu et al., 2019). Multiple studies in freshwater ecosystems have indicated relationships (both positive and negative) between organic matter, mercury loading, methylation, and biomagnification (Bravo et al., 2018; Lavoie et al., 2013). Land use has also been indicated as a factor influencing Hg bioaccumulation, with loons (*Gavia immer*) showing increased blood Hg in lakes surrounded by shrubland or wetlands and decreased in agricultural systems (Kramar et al., 2005) and with walleye (*Sander vitreus*) best predicted by habitat and watershed features rather than water chemistry (Hayer et al., 2011). In lakes, human land use has been associated with declines in Hg in fish in contrast with forested watersheds where fish Hg concentrations are higher (Chen et al., 2005). However, still other studies have shown fewer clear-cut linkages between bioaccumulation and Hg sources, land use, or biogeochemistry (Eagles-Smith et al., 2016a; Kamman et al., 2005). Insights gained from these studies may not translate directly to estuarine and marine ecosystems even though general patterns of influence on bioaccumulation may help predict important factors to consider (e.g. land use or organic carbon).

These past meta-analyses of freshwater ecosystems, while capturing a range of abiotic and biotic conditions, have typically not included Hg contaminated sites, which are often found in coastal and estuarine environments. Hg loading, fate, and bioaccumulation in contaminated estuarine systems are particularly important to understand given the elevated risk posed to human and wildlife health and the need for remediation of the sites. The Hg sources and sediment concentrations at contaminated sites differ from relatively unimpacted areas, yet comparisons of the processes driving Hg transformation and fate between contaminated and uncontaminated sites have rarely been investigated (but see (Seelen et al., In Press)). Our past research in a range of estuarine systems has indicated that large variability exists in bulk sediment concentrations (classically considered to be the primary source of MeHg to aquatic systems) and in the water column but variability in resident fish tissue concentrations is much lower (Buckman et al., 2017; Chen et al., 2014; Taylor et al., 2019). Contaminated sites in US estuaries (e.g. Lavaca Bay, TX; Penobscot River, ME; Berry's Creek, NJ) have, on average, higher sediment concentrations and thus, decisions about their remediation largely focus on the sediment compartment. But given the physical and chemical dynamics of estuaries which experience daily tidal fluxes and resuspension in the water column, the consideration of the influence of benthic-pelagic coupling is particularly important in understanding the fate of Hg in their food webs. Higher sediment concentrations do not always result in high fish concentrations (Buckman et al., 2017; Chen et al., 2009), particularly at sites without a known contamination source. Similarly, studies have found stronger relationships between surface water concentrations and biota than between bulk sediment and biota (Buckman et al., 2019; Chen et al., 2014; Taylor et al., 2019). Small scale influences of land use on Hg cycling have also been observed. For example, urban development has been associated with greater loading of Hg (e.g. Buckman et al., 2017) and salt marshes, with enhanced methylation potential, are both a source and sink for particulate MeHg depending upon conditions (Bergamaschi et al., 2012; Mitchell and Gilmour, 2008; Mitchell et al., 2012; Shi et al., 2018; Turner et al., 2018). However, these patterns in bioaccumulation on

small scales (within site or within system) may or may not scale up to larger regional and global scales given the complexity of estuarine dynamics on both spatial and temporal scales.

Forage fish provide a critical link to transfer MeHg from primary producers and consumers to larger fish which are consumed by humans. The mummichog (*Fundulus heteroclitus*) and the Atlantic silverside (*Menidia menidia*) are ubiquitous in Northeast US estuaries and are important links in the trophic nekton relay (Kneib, 2000), facilitating the movement and export of carbon and contaminants through estuaries. The two species display different ecological characteristics, with *Fundulus* a year round estuarine resident whose feeding ecology links benthic and pelagic systems and adult *Menidia* overwintering offshore and feeding pelagically (Conover and Murawski, 1982; Fry et al., 2008; Griffin and Valiela, 2001; McMahon et al., 2005). They are abundant and easy to collect, are relatively well understood ecologically, and are important prey species for larger fish. These and other characteristics of both species make them useful for monitoring MeHg uptake and trophic transfer, with *Fundulus* identified as a key species for large scale bio-monitoring in the Northeast US (Evers et al., 2008).

Our research in estuarine environments has provided an opportunity to use a large regional dataset collected from 2012 to 2016 to explore the relationships between land use, water, and sediment characteristics and forage fish mercury concentrations. Using data gathered across multiple systems in the Northeast US, we address the following objectives: examine whether benthic or pelagic processes have a greater influence on bioaccumulation across sites, systems, and species; investigate the influence of known Hg sediment contamination on exposure pathways and tissue concentrations; and explore within-system versus across-system similarities in relationship between fish Hg and environmental variables. We have previously observed pelagic concentrations to be of greater importance to predicting fish concentrations (e.g. (Chen et al., 2014)) but it is unknown whether this pattern is consistent within a larger data set containing more sites and a greater range of Hg concentrations. Seelen et al. (In Press) found evidence that abiotic processes driving MeHg concentration in the water column are fundamentally different between contaminated and uncontaminated sites. These different processes have the potential to directly or indirectly affect bioaccumulation and tissue concentrations in forage fish. Along with differences between contaminated and uncontaminated sites, we expect that data will cluster by system (e.g. sites from Delaware River estuary will cluster with other Delaware sites, rather than sites from a Maine estuary system), anticipating that bioaccumulation would be driven by loading as well as productivity and water column processes, which we again expect to be more similar within a watershed system than between geographically disparate sites and systems. Through this combined dataset and analysis, we provide a more synthetic understanding of the processes influencing Hg and MeHg bioaccumulation in estuarine food webs, and discuss the topics posed above.

2. Methods

2.1. Sample collection and analysis

Sample sites, collection methods, and abiotic sample analyses have been described in Seelen et al. (In Press). Briefly, 38 sites in 8 systems were sampled between 2012 and 2016 and included in this analysis (Fig. 1). Systems were defined by the major aquatic geographical feature near the sites (usually a river or bay) and include the Delaware Bay (14 sites), Chesapeake Bay (4 sites), Long Island Sound (4 sites), Webhannet River (4 sites), Penobscot River (2 sites), Berry's Creek (3 sites), Hackensack River (3 sites), and Mt. Desert Island (4 sites). Data from 2012 were previously published in Buckman et al. (2017) and from 2013 in Taylor et al. (2019). Abiotic data utilized in this analysis are a subset of the data in Seelen et al. (In Press). 2015 and 2016 fish data have not been previously published.

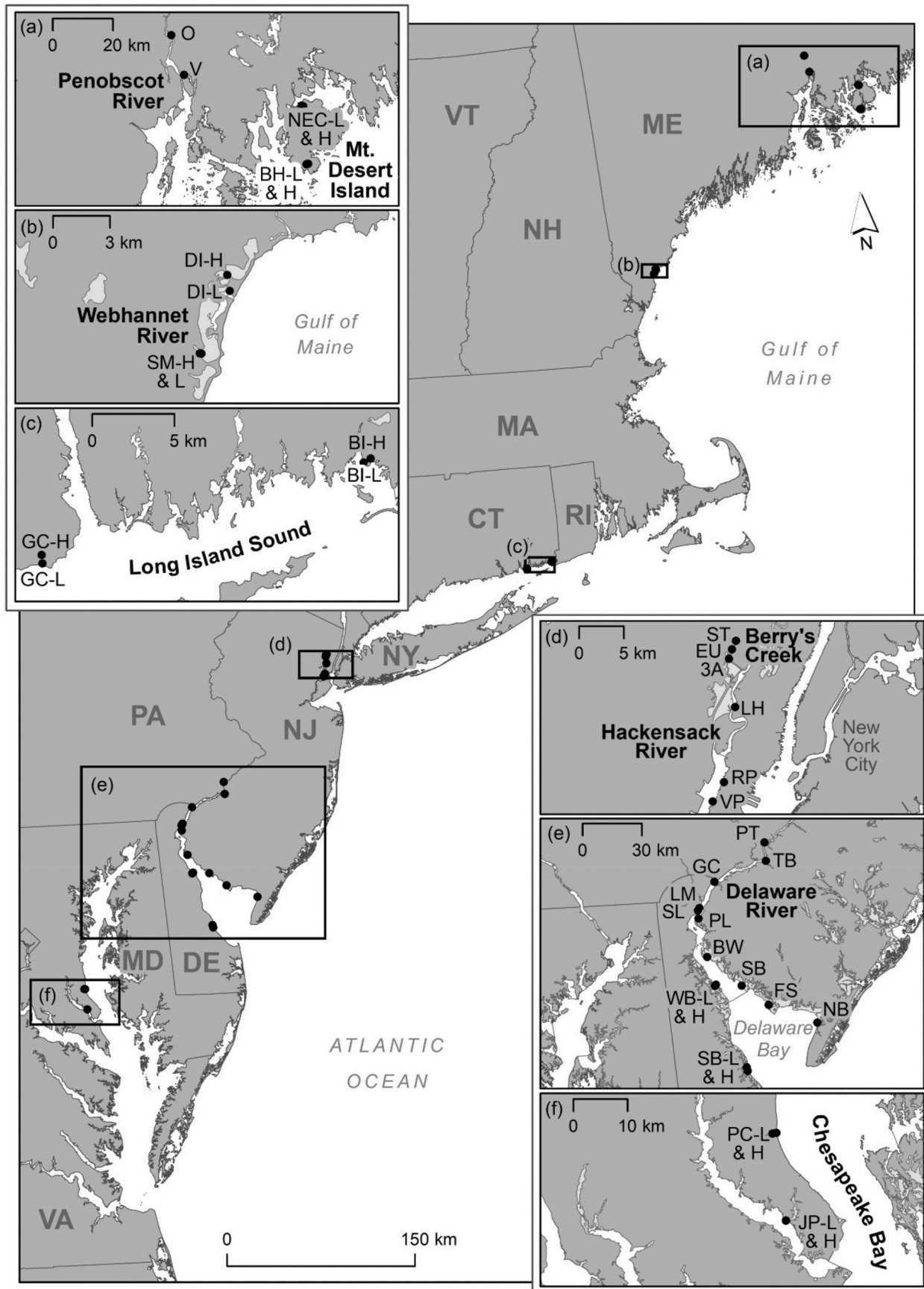


Fig. 1. Map of all sampling sites with insets indicating sites in a) Penobscot River and Mt. Desert Island systems, b) Webhannet River system, c) Long Island Sound, d) Hackensack River and Berry's Creek, e) Delaware River estuary, and f) Chesapeake Bay. Site codes for each site are indicated in the insets.

2.1.1. Sediment

Sediment samples consisted of the top 2–4 cm of sediment and were collected subtidally at low tide through grab samples or sediment cores. All sediment and water analyses were conducted by members of the Mason Lab at the University of Connecticut Dept of Marine Sciences or Umeå University in Sweden. Detailed descriptions of analytical methods for sediment and water data are available in Buckman et al. (2017), Taylor et al. (2019), and Seelen et al. (In Press) for collection years 2012, 2013, and 2015 and 2016 respectively. Generally, MeHg was extracted from freeze-dried sediments by aqueous distillation extraction (H_2O , KCl, H_2SO_4) (Horvat et al., 1993; Hammerschmidt and Fitzgerald, 2001), ethylated ($(\text{C}_2\text{H}_5)_4\text{BNa}$) and measured on a Tekran 2700 Automated Methylmercury Analysis System that makes use of purge and trap gas chromatography-cold vapor atomic fluorescence spectrometry (GC-CVAFS) (Hammerschmidt and Fitzgerald, 2006). MeHg spike recoveries averaged 101% for 2012 samples (Buckman et al., 2017), 96% for 2013 samples (Taylor et al., 2019), and 114% for 2015 and 2016 samples combined (Seelen et al., In Press). Total mercury (THg) was measured by Direct Mercury Analyzer (Milestone DMA-80 or MA 3000 depending upon the year) with SRM recoveries of 99% for 2012 (Buckman et al., 2017), 95% for 2013 samples (Taylor et al., 2019) and 102% for 2015 and 2016 (Seelen et al., In Press). More detailed QA/QC for all abiotic analyses are available in the referenced publications. Organic carbon content was approximated as percent loss on ignition (% LOI) via combustion at 550 degrees C.

2.1.2. Water Column

Water samples were collected at either high or rising tide using trace metal clean techniques, and were filtered within 12 h in a laminar flow hood using a pre-combusted quartz fiber filter. Filters were analyzed for total suspended solids (TSS), particulate MeHg, and particulate THg, while filtrate subsamples were appropriately preserved and analyzed for MeHg and THg and dissolved organic carbon (DOC), nitrate, nitrite (Shimadzu TOC/TN analyzer). Water was also filtered for chlorophyll a (chl_a) and phaeopigment (pha) using GF/F filters and analyzed via acetone extraction and acidification. Pha was not analyzed for Delaware 2012 samples and concentrations were instead estimated from similar sites (Gosnell et al., 2016). Particulate MeHg was extracted from the filters by digestion (HNO_3), neutralization (KOH and $\text{C}_2\text{H}_3\text{O}_2$ buffer) and ethylation prior to GC-CVAFS analysis using the Tekran 2700 as for the sediments. Dissolved MeHg samples were digested utilizing H_2SO_4 and L-ascorbic acid prior to ethylation, but otherwise was analyzed similarly (Hammerschmidt and Fitzgerald, 2001; Munson et al., 2014). Particulate THg filters were digested with HNO_3 and BrCl and dissolved THg samples with only BrCl prior to reduction with hydroxylamine hydrochloride and stannous chloride and then CVAFS analysis (Tekran 2600). Water column THg recoveries averaged 101% for 2012 samples (Buckman et al., 2017), 97% for 2013 samples (Taylor et al., 2019), and 121% (particulate) and 76% for 2015 and 2016 samples (Seelen et al., In Press). MeHg distillation spike recoveries averaged 93% for 2012 samples (Buckman et al., 2017), 115% for 2013 samples (Taylor et al., 2019), and 103% (particulate) and 86% (dissolved) for 2015 and 2016 analyses (Seelen et al., In Press). Ancillary water column data including temperature, pH, salinity, dissolved oxygen, and conductivity were measured *in situ* using a handheld sonde (Hydrolab MS5). Land cover class proportions (%) were calculated within the US Geological Survey (USGS) Watershed Boundary Dataset (WBD) Hydrologic Unit Code 12 (HUC-12) sub-watershed polygons in ArcGIS. Land cover data were obtained from the 2011 National Land Cover Database (Homer et al., 2015). Area occupied by water was subtracted so that the land cover class proportions were based on terrestrial area only, as many coastal sites included significant estuarine area within the HUC-12 sub-watershed boundaries.

2.1.3. Biota

Forage fish were collected using a hand-held seine, euthanized on

site, and frozen for transport back to the lab. All collections were undertaken with appropriate permits, and utilizing protocols approved by the Dartmouth Institutional animal care and use committee. In the laboratory, whole individual fish were rinsed with ultra-pure water (18MOhm), total length measured, weighed for wet weight, freeze-dried (Labconco Freezone 4.5) in a trace-metal free glass vial, reweighed for dry weight, and snipped to a fine powder using acid-rinsed ceramic scissors. Whole individuals were used for analysis (*Fundulus* %moisture = $76 \pm 3\%$; *Menidia* %moisture = $78 \pm 4\%$). *Fundulus* for all years were analyzed for MeHg concentration by species specific isotope dilution ICP-MS using a MERX-M automated methylmercury analyzer coupled to an ICP-MS (Element 2 for analysis prior to 2014, Agilent 7900 for analysis after 2014). *Menidia* from 2012, 2013, and 2015 were analyzed via Hg speciation as above and resulting MeHg and inorganic Hg measurements summed for THg. A subset of samples were analyzed by DMA to verify that the sum of the species (MeHg + inorganic Hg) was equivalent to total Hg. *Menidia* from 2016 were analyzed for THg by Milestone 80 DMA. Average %MeHg for all individuals undergoing Hg speciation was 95% in *Menidia* (Table S3), thus THg is an adequate proxy for MeHg in this species and was utilized for statistical analysis as it allowed for greater sample numbers. If an individual was analyzed both via Hg speciation and DMA, the concentration determined via DMA was preferentially used for statistical analyses. All biotic analyses were completed at the Dartmouth Trace Element Analysis Core. MeHg average percent recovery(s.d) of SRMs for Hg speciation analyses of 2015 and 2016 samples were 85% (0.07) for DORM4 and 108% (0.03) for TORT2. Recovery of standards analyzed for THg via DMA were 70% (TORT2) and 106% (DOLT4). Previously published QA/QC for biotic analyses are summarized in Table S1.

2.2. Statistical analysis

Statistical analyses were carried out using JMP Pro 14 (SAS). Individual fish measurements were retained for analysis, however, average sediment and water (when not a single measurement) concentrations were calculated for each site to pair with individual fish concentrations. For the sites which were sampled in multiple years, abiotic concentrations were averaged by year. Gaussian mixture models cluster analysis was employed to explore the relationships between biotic and abiotic mercury concentrations, ancillary environmental variables, and land use across the various sites and systems. In JMP, the “normal mixtures” option was chosen from the cluster menu. Normal mixtures cluster analysis is a type of unsupervised machine learning that assumes data come from overlapping multivariate normal distributions. It performs a “soft” classification, assigning a probability of being in each cluster to each data point (i.e. each individual fish). It accounts for variance and is more robust to bias of unequal cluster sizes and overlapping clusters, unlike k-means clustering. JMP utilizes a Bayesian Expectation Maximization (EM) algorithm to fit the distributions, iteratively running multiple independent restarts with independent estimates for the cluster centers and parameters. The results indicate clusters with data points assigned to each cluster based on the highest probability of sharing common characteristics. This method was chosen as it allows for visualization of commonalities in the data set, without the bias of *a priori* labels or hypothesized relationships. Each fish species was run separately, as this allowed for inclusion of more sites for *Fundulus*, and previous analyses have indicated significant differences in MeHg concentrations between the two species within sites. In the current data set, Welch’s ANOVA comparing MeHg between species using only sites where both were present also indicates a difference ($F=18.6$, $p<0.0001$). The environmental data included in the model were particulate THg and MeHg, total suspended solids (TSS), dissolved THg and MeHg, DOC, chl_a, chl_a:pha, nitrate, salinity, sediment THg, MeHg, and %LOI, and HUC-12 land use estimates. Concentration data were log₁₀ transformed and proportion data (e.g. land use, LOI) were logit transformed prior to analysis. Similar land use categories were combined to

result in broad use categories of no-low development, med-high development, forest, wetland, and agriculture (e.g. cropland + pasture=agriculture). *Fundulus* MeHg concentration data were normalized to a standard length of 65 mm prior to analysis. This was accomplished by running a mixed model with length as the fixed variable and system (e.g. Hackensack, Delaware) and system*length as random variables. The conditional predicted value (taking fixed and random effects into account) was calculated for a 65 mm fish, and the residual added to the predicted value to generate length normalized and standardized (LNST) MeHg concentrations for each individual fish as per [Eagles-Smith and Ackerman \(2014\)](#). *Menidia* did not indicate significant length:concentration effects when running the model, thus log₁₀ THg of the measured values were utilized for the cluster analysis without length normalization and standardization.

The cluster analysis was run for each species separately using the “Normal Mixture” option in JMP, with parameters of 500 tours (number of independent restarts), 1500 maximum iterations (maximum number of iterations in the convergence phase), a 1e-8 convergence criterion (difference in likelihood when EM terminates), and estimated 2–15 clusters with an outlier cluster (this option is less sensitive to perturbation by multivariate outliers). The best cluster arrangement was chosen by the lowest Bayesian Information Criterion (BIC) and correlation matrices for each cluster were automatically generated by the algorithm. Due to the nature of the normal means algorithm, each individual processing run may result in a slightly different cluster arrangement. We present the results of one run (500 independent starts) of the algorithm, and anticipate similar though not exact groupings for other runs due to the independent estimates of starting cluster parameters.

3. Results

3.1. Variable values and ranges

Variables included within the analysis exhibited a large variability across sites ([Tables 1 and S2](#)). Site averages of sediment THg ranged from 0.85 to 36034 ng/g DW, sediment MeHg from 0.01 to 62.5 ng/g DW, and organic carbon from 1 to 26% LOI. Relatively elevated sediment mercury concentrations were within the Berry's Creek (NJ), Hackensack River (NJ), and Penobscot River (ME) systems ([Table 1](#)). There were no geographic patterns observed across systems for %LOI, due in part to sample campaigns targeting high and low carbon environments within the same watershed in MD, DE, CT, and ME. Water column mercury was similarly variable, with dissolved concentrations of THg ranging from 0.2 to 11.9 ng/L and MeHg from 0.002 to 1.15 ng/L. Particulate THg ranged from 1.9 to 3433 ng/g DW, MeHg from 0.1 to 36 ng/g DW, and TSS from 3.1 to 163 ng/L. Typically, highest water column concentrations were found within the Berry's Creek system, with relatively higher dissolved MeHg also observed within Mt. Desert Island (ME) sites and at Barn Island (CT) in Long Island Sound. Overall, there was a larger range in sediment Hg and MeHg than for the water column, with dissolved Hg and MeHg showing least variation.

For the current sites, *Fundulus* MeHg concentration ranged from 6 to 1465 ng/g DW across 295 individuals from 36 sites ([Table 2](#)). One site (GC-L from 2015) was not included in the cluster analysis for either species due to missing water column mercury concentrations. This eliminated 5 individuals for *Fundulus*. *Menidia* THg concentration ranged from 15 to 1982 ng/g DW across 198 individuals from 27 sites (5 of these individuals not included in cluster analysis due to missing water column data). Tissue concentration range was most similar to dissolved MeHg, with hundreds-fold differences as opposed to thousands-fold differences for sediment Hg and MeHg. For both species, individuals from Berry's Creek had the highest tissue concentrations, with elevated concentrations also observed in the Hackensack River (both species) and Penobscot River and some individual sites in the upper Delaware for *Fundulus*. Most sites had tissue concentrations near or below 200 ng/g

DW. Average %MeHg for *Fundulus* was above 80% for all systems ([Table S3](#)), though statistical analyses were conducted on MeHg concentration rather than THg for this species due to variability. For *Menidia*, %MeHg is usually greater than 90% with less variability than previously observed for *Fundulus*, so THg is an adequate proxy for *Menidia* MeHg concentration ([Table S3](#)).

Ancillary water column variables also exhibited large ranges: DOC 1.3–28.46 mg/L (all but 3 sites were below 10 mg/L); salinity 0–33; chl_a 1.7–74 µg/L; chl:pha 0.3–324; and nitrate 0.01–1113 µg/L ([Table S2](#)). Nitrate was highest in the Delaware River (PA, DE, NJ), Hackensack River and Berry's Creek systems, with individual sites within these same systems exhibiting the highest chlorophyll concentrations. Development ranged from 3 to 51% for no to low development and 0–86% for medium to high development sites, with greatest urbanization observed in the Berry's Creek and Hackensack systems in NJ, and portions of the upper Delaware River and Long Island Sound systems ([Figure S1](#)). Forested landscapes ranged from 0 to 76% cover, with most forested sites in the Maine estuarine systems and portions of Long Island Sound. In contrast, agriculture (range 0–36%) and wetland (range 0–79%) landscapes were most prevalent at the Delaware River sites included in this analysis ([Table S2](#)).

3.2. Normal means clustering analysis

For *Fundulus*, data from all sites indicated 6 clusters with no individual fish in an outlier cluster, while the reduced model, with no contaminated sites included, resulted in 5 clusters with 5 individuals from one site in the Delaware in an outlier cluster ([Figs. 2 and 4](#)). *Menidia* data from all sites formed 5 clusters, also with no individuals in the outlier cluster, while the reduced model formed 4 clusters with 3 individuals in an outlier cluster ([Figs. 2 and 6 and S2](#)). We had hypothesized that clusters would most likely form by system, with system-wide variables being both more similar to each other and the more important drivers of bioaccumulation than broader scale regional patterns across system. Yet, this was not the case for either fish species, with fish from sites within the same system grouped into different clusters for both the whole and uncontaminated models ([Fig. 2](#)).

3.2.1. *Fundulus*

For all sites combined, each cluster revealed particular relationships between *Fundulus* MeHg concentration and environmental and land-use variables through correlations ([Fig. 3](#)). Cluster 1 (44 individuals) was defined by strong ($0.6 < |r| > 1.0$) positive correlations with both water and sediment THg and MeHg, LOI, nitrate, TSS, and high levels of development, with strong negative correlations with forested land cover within the watershed. Cluster 2 (58 individuals) indicated strong positive associations with dissolved THg and MeHg, particulate THg, sediment THg and MeHg, %LOI, and development with strong negative associations with salinity, DOC, forest, and agriculture. Cluster 3 did not indicate strong negative or positive correlations between tissue concentration and any of the other variables, with moderate ($0.4 < |r| > 0.6$) negative correlations with agriculture and wetlands (59 individuals). Cluster 4 (35 individuals) shows strong correlations between tissue MeHg and water column and sediment THg and MeHg, chl:pha, and high development, moderate positive correlations with DOC and low development, and strong negative correlations with forest and agriculture. The land use association contrast with those observed in freshwater systems in which Hg in fish tissue had positive correlations with forest cover ([Chalmers et al., 2014](#); [Chen et al., 2005](#)). The fish in cluster 5 are strongly positively correlated with water column THg, sediment THg and MeHg, chl:pha, and moderately positively correlated with DOC, while strongly negatively correlated with salinity, and moderately negatively correlated with TSS, development, and wetland cover (47 individuals). The final cluster (47 individuals) indicates only a strong negative correlation with forest cover in the watershed. Two thirds of the clusters indicate strong relationships between tissue concentrations

Table 1

MeHg and THg concentrations by site used for normal means cluster analysis. Sediment concentrations are an average of multiple samples. Range and sample sizes for sediment data are available in [Seelen et al. \(in press\)](#). Ancillary water column and land use values are in [Supplemental Table S2](#).

system	site code	sample year	Sediment MeHg (ng/g DW)	Sediment THg (ng/g DW)	Diss. MeHg (ng/L)	Diss. HgT (ng/L)	Part. MeHg (ng/g)	Part. HgT (ng/g)	Source
Berry's Creek	3A	2016	7.5	2378.3	0.3	5.1	9.2	1198.0	Seelen et al. (in press)
Berry's Creek	EU	2016	62.5	36034.1	0.5	9.2	22.0	3433.4	Seelen et al. (in press)
Berry's Creek	ST	2016	37.0	14084.8	0.6	11.9	35.9	3032.3	Seelen et al. (in press)
Chesapeake	JP-H	2013	0.02	1.9	0.01	0.3	2.8	46.0	Taylor et al. (2019)
Chesapeake	JP-L	2013	0.02	0.9	0.04	0.4	1.1	35.3	Taylor et al. (2019)
Chesapeake	PC-H	2013	0.3	48.1	0.01	0.3	0.5	25.1	Taylor et al. (2019)
Chesapeake	PC-L	2013	0.01	1.2	<0.01	0.4	0.2	19.4	Taylor et al. (2019)
Delaware River	BW	2012	4.9	114.0	0.1	0.6	1.0	112.5	Buckman et al. (2017)
Delaware River	FS	2012	0.2	60.7	0.1	0.4	1.6	72.4	Buckman et al. (2017)
Delaware River	GC	2012	1.5	262.0	0.1	0.5	0.3	58.4	Buckman et al. (2017)
Delaware River	LM	2012	0.8	564.8	0.04	0.5	1.0	131.9	Buckman et al. (2017)
Delaware River	NB	2012	0.1	49.2	0.01	0.9	1.9	95.0	Buckman et al. (2017)
Delaware River	PL	2012	0.2	256.2	<0.01	0.7	0.7	126.5	Buckman et al. (2017)
Delaware River	PT	2012	1.6	272.6	0.01	0.2	0.3	155.3	Buckman et al. (2017)
Delaware River	SB	2012	2.8	68.5	0.02	0.6	0.6	36.2	Buckman et al. (2017)
Delaware River	SB-H	2015	2.6	155.0	0.03	2.6	1.5	35.1	Seelen et al. (in press)
Delaware River	SB-L	2015	0.4	34.8	0.02	1.6	1.3	35.5	Seelen et al. (in press)
Delaware River	SL	2012	0.8	299.0	0.1	0.5	2.8	365.6	Buckman et al. (2017)
Delaware River	TB	2012	0.4	84.2	<0.01	0.3	0.6	232.1	Buckman et al. (2017)
Delaware River	WB-H	2015	3.2	266.8	0.02	1.4	0.5	81.7	Seelen et al. (in press)
Delaware River	WB-L	2015	0.4	16.7	0.02	1.2	0.7	44.0	Seelen et al. (in press)
Hackensack River	LH	2016	23.6	2209.3	0.1	2.4	2.8	388.1	Seelen et al. (in press)
Hackensack River	RP	2016	1.9	142.5	0.2	1.7	6.9	428.5	Seelen et al. (in press)
Hackensack River	VP	2016	2.0	364.8	0.02	0.9	1.5	430.7	Seelen et al. (in press)
Long Island Sound	BI-H	2013	0.1	65.6	0.5	1.7	22.6	113.2	Taylor et al. (2019)
Long Island Sound	BI-H	2015	0.2	72.8	0.1	1.2	2.3	31.7	Seelen et al. (in press)
Long Island Sound	BI-L	2013	0.3	6.8	0.3	1.1	17.0	99.8	Taylor et al. (2019)
Long Island Sound	BI-L	2015	0.4	11.5	0.03	0.8	0.7	12.3	Seelen et al. (in press)
Long Island Sound	GC-H	2013	0.1	107.3	0.03	0.4	0.7	25.2	Taylor et al. (2019)
Long Island Sound	GC-H	2015	0.2	175.7	0.03	1.4	0.6	25.9	Seelen et al. (in press)
Long Island Sound	GC-L	2013	0.2	29.0	0.02	0.3	0.5	19.8	Taylor et al. (2019)
Mt. Desert Island	BH-H	2013	0.2	139.9	1.1	3.9	6.7	71.5	Taylor et al. (2019)
Mt. Desert Island	BH-L	2013	0.4	102.7	0.1	1.0	4.5	86.5	Taylor et al. (2019)
Mt. Desert Island	NEC-H	2013	1.6	60.1	0.5	1.9	3.4	21.5	Taylor et al. (2019)
Mt. Desert Island	NEC-L	2013	0.5	30.1	0.5	1.8	3.2	20.9	Taylor et al. (2019)
Penobscot River	O	2016	35.4	986.6	0.05	1.7	7.2	308.1	Seelen et al. (in press)

(continued on next page)

Table 1 (continued)

system	site code	sample year	Sediment MeHg (ng/g DW)	Sediment THg (ng/g DW)	Diss. MeHg (ng/L)	Diss. HgT (ng/L)	Part. MeHg (ng/g)	Part. HgT (ng/g)	Source
Penobscot River	V	2016	19.2	520.7	0.02	1.3	1.3	101.2	Seelen et al. (in press)
Webhannet River	DI-H	2015	0.4	16.4	<0.01	0.3	0.1	1.9	Seelen et al. (in press)
Webhannet River	DI-L	2015	0.1	5.9	<0.01	0.3	0.6	18.6	Seelen et al. (in press)
Webhannet River	SM-H	2015	1.0	31.0	0.02	0.5	0.4	13.4	Seelen et al. (in press)
Webhannet River	SM-L	2015	0.3	9.9	0.03	0.5	1.0	16.1	Seelen et al. (in press)

and both sediment and water column Hg concentrations for *Fundulus*. This contrasts with our previous estuarine studies that have found weaker relationships with sediment concentrations for this species (Buckman et al., 2017; Chen et al., 2014; Taylor et al., 2019) but is similar to findings in urban coastal lagoons (Chen et al., 2021).

The four clusters indicating stronger sediment-tissue correlations all contain sites with known nearby sources of Hg contamination to the estuary as well as relatively unimpacted sites (Fig. 4a) suggesting that the large variation in sediment Hg and MeHg within these clusters is highly influential. When sites with high sediment loading (indicated by sediment THg >400 ng/g) were removed, the relationship of sediment to *Fundulus* tissue concentration is less dramatic (Figs. 3b and 4). Without contaminated sites, two clusters (3 and 5; note that these do not contain the same sites as the whole model clusters (Fig. 2)) show the strongest correlations between sediment and *Fundulus* tissue concentrations relative to the other clusters in the model (Fig. 4b). Cluster 1 fish (35 individuals) are strongly positively correlated with dissolved and sediment THg, and moderately positively correlated with dissolved MeHg, DOC, particulate Hg, sediment MeHg, and LOI. Cluster 2 fish (37 individuals) are strongly correlated with DOC, moderately positively correlated with dissolved and particulate THg, and moderately negatively correlated with salinity and development. Cluster 3 (91 individuals) indicates strong positive relationships with dissolved THg, DOC, wetlands, and sediment Hg, and a strong negative relationship with chl. Moderate positive correlations were observed with dissolved MeHg, TSS, and LOI and moderate negative correlations with chl:pha and agriculture. Cluster 4 fish (31 individuals) are positively correlated with dissolved THg and moderately correlated with DOC, TSS, chl:pha (positive) and forest (negative). The final cluster for *Fundulus* from uncontaminated sites is strongly positively correlated with sediment THg, and moderately positively correlated with particulate THg, development and sediment MeHg (54 individuals). Negative moderate correlations were observed with forest and agriculture as in some of the whole model clusters.

3.2.2. *Menidia*

Menidia from all sites combined separated into five clusters with no individuals in the outlier cluster. The first cluster (27 individuals) indicated strong positive correlations between fish THg (proxy for MeHg) and water column (both dissolved and particulate fractions) MeHg and THg (Fig. 5A). There were moderate positive correlations with chl, and moderate negative correlations with forest, salinity, low development, and chl:pha. The second cluster (30 individuals) also indicated strong positive correlations with dissolved MeHg and THg, as well as particulate MeHg, and moderate positive correlations with salinity, high development, and sediment MeHg. There were no strong negative associations in the second cluster. The third *Menidia* cluster was characterized by strong positive correlations with dissolved MeHg and THg, particulate THg, high development, sediment MeHg and THg, and moderate positive correlations with DOC, particulate MeHg, chl:pha, and nitrate. Agriculture and forest cover were strongly negatively associated with fish THg concentrations (41 individuals). 53 individuals made up the fourth cluster, with fish concentrations strongly positively

correlated with dissolved and particulate THg and MeHg, and DOC; and moderately negatively correlated with agriculture, chl, and chl:pha. In the final cluster, there were no strong relationships between *Menidia* THg concentrations and any of the other variables (48 individuals).

The most prevalent pattern across all clusters is the strong positive relationship of tissue Hg with water column Hg concentrations, particularly dissolved THg and MeHg, and the relative lack of relationship with bulk sediment Hg relative to what was observed for *Fundulus* (Fig. 6, Figure S2).

Removal of contaminated sites only eliminated 2 sites and 10 individuals from the analysis for *Menidia*, yet differences in clusters and correlations within each cluster relative to the full model were still observed (Figs. 2 and 5). *Menidia* from only uncontaminated sites separated into four clusters with three individuals from Pennsville Landfill (Delaware River) in an outlier cluster. Clusters 1 through 3 indicated strong positive relationships between fish THg and dissolved THg and for clusters 1 and 2, also indicating a strong positive relationship with dissolved MeHg, similar to broad patterns in the full site model (Fig. 5B and S2). Cluster 1 (42 individuals) also indicated a strong positive relationship with particulate MeHg, and moderate relationships with particulate THg (positive) and chl:pha (negative). There were no strong correlations with land use or sediment for this cluster. Cluster 2 (38 individuals) indicated strong positive relationships between tissue THg and salinity, sediment THg, and %LOI along with dissolved THg and MeHg. There were moderate positive relationships between tissue concentration and DOC, particulate THg and MeHg, and sediment MeHg. Like Cluster 1 for uncontaminated *Menidia*, there were weak positive relationships with development and weak negative relationships with forest and agriculture. Cluster 3 (49 individuals) exhibited strong positive relationships between dissolved THg, DOC, salinity, and chl:pha and tissue concentrations, moderate positive relationships with dissolved MeHg, TSS, particulate MeHg, and % wetland, and a moderate negative relationship with % forest in the sub-watershed. Cluster 4 (51 individuals) did not exhibit strong relationships between tissue concentration and any of the abiotic variables. There were moderate positive correlations between fish and dissolved MeHg, particulate THg and MeHg, med-high development, and sediment MeHg and moderate negative correlations with forest, agriculture, and wetland. This cluster contained one site from the Hackensack River that had noticeably higher fish tissue concentrations than any of the other uncontaminated sites, and may be highly influential on the correlations.

4. Discussion

Three main themes influencing forage fish patterns of Hg concentration were revealed by the cluster analyses and correlations. Tissue concentrations are closely related to abiotic Hg, with the importance of bulk sediment as a predictor of bioaccumulation increasing at contaminated sites for *Fundulus*, and for *Menidia* to a lesser degree. Species-specific feeding ecology is relevant to these exposure pathways, with *Fundulus* being linked to both benthic and pelagic sources of MeHg and *Menidia* representative of mostly pelagic sources of MeHg. Additionally,

Table 2

Forage fish MeHg and THg concentrations by site and species. Fish length values and %MeHg are available in [Supplemental Table S3](#). LNST denotes MeHg concentration length normalized and standardized to a 60 mm fish.

system	site code	sample year	<i>Fundulus heteroclitus</i>			<i>Menidia menidia</i>			Data Source	
			mean \pm st. dev. MeHg (ng/g DW)	range MeHg (ng/g DW)	n	mean \pm st. dev. MeHg LNST (ng/g DW)	mean \pm st. dev. THg (ng/g DW)	range THg (ng/g DW)		n
Berry's Creek	3A	2016	658 \pm 192	502–931	5	437 \pm 159	1380 \pm 384	1032–1982	5	
Berry's Creek	EU	2016	830 \pm 498	332–1465	5	534 \pm 286				
Berry's Creek	ST	2016	851 \pm 284	565–1237	5	478 \pm 188				
Chesapeake	JP-H	2013	26 \pm 23	7–118	27	26 \pm 15	48 \pm 48	23–166	8	Taylor et al. (2019)
Chesapeake	JP-L	2013	31 \pm 9	13–50	19	26 \pm 9	48 \pm 25	15–90	12	Taylor et al. (2019)
Chesapeake	PC-H	2013	18 \pm 4	11–24	5	15 \pm 3	28 \pm 19	15–76	17	Taylor et al. (2019)
Chesapeake	PC-L	2013	27 \pm 5	23–31	4	23 \pm 4	33 \pm 10	24–49	5	Taylor et al. (2019)
Delaware River	BW	2012	61 \pm 16	47–83	4	49 \pm 15				Buckman et al. (2017)
Delaware River	FS	2012	44 \pm 13	20–61	12	46 \pm 10	77 \pm 21	59–107	4	Buckman et al. (2017)
Delaware River	GC	2012	50 \pm 8	41–57	3	87 \pm 11				Buckman et al. (2017)
Delaware River	LM	2012	123 \pm 57	83–245	7	117 \pm 50				Buckman et al. (2017)
Delaware River	NB	2012	89 \pm 141	19–489	10	87 \pm 115	59 \pm 2	58–61	3	Buckman et al. (2017)
Delaware River	PL	2012	91 \pm 23	59–128	6	85 \pm 17	64 \pm 15	54–82	3	Buckman et al. (2017)
Delaware River	PT	2012	121 \pm 59	68–208	5	105 \pm 37				Buckman et al. (2017)
Delaware River	SB	2012	48 \pm 28	18–88	7	59 \pm 38	69 \pm 8	60–77	3	Buckman et al. (2017)
Delaware River	SB-H	2015	103 \pm 35	76–162	5	107 \pm 46	101 \pm 20	82–133	5	
Delaware River	SB-L	2015					100 \pm 26	72–129	5	
Delaware River	SL	2012	130 \pm 57	57–261	14	133 \pm 56				Buckman et al. (2017)
Delaware River	TB	2012	59 \pm 21	13–89	9	56 \pm 21				Buckman et al. (2017)
Delaware River	WB-H	2015	111 \pm 30	81–156	5	111 \pm 30	72 \pm 15	60–90	5	
Delaware River	WB-L	2015	153 \pm 49	95–217	5	157 \pm 47	85 \pm 7	73–91	5	
Hackensack River	LH	2016	410 \pm 86	276–492	5	297 \pm 87	267 \pm 146	188–529	5	
Hackensack River	RP	2016	317 \pm 49	270–390	5	265 \pm 32	858 \pm 269	538–1140	5	
Hackensack River	VP	2016					126 \pm 42	89–188	5	
Long Island Sound	BI-H	2013	42 \pm 15	29–66	5	55 \pm 19	169 \pm 19	153–190	5	Taylor et al. (2019)
Long Island Sound	BI-H	2015	50 \pm 26	24–85	5	48 \pm 26	157 \pm 58	84–241	5	
Long Island Sound	BI-L	2013					179 \pm 44	119–241	5	Taylor et al. (2019)
Long Island Sound	BI-L	2015	130 \pm 34	82–161	5	122 \pm 24	185 \pm 22	164–217	5	
Long Island Sound	GC-H	2013	14 \pm 6	8–21	5	17 \pm 5	70 \pm 11	50–80	5	Taylor et al. (2019)
Long Island Sound	GC-H	2015	46 \pm 11	35–64	5	45 \pm 7	99 \pm 24	66–130	5	
Long Island Sound	GC-L	2013	14		1	33	103 \pm 34	79–163	5	Taylor et al. (2019)
Mt. Desert Island	BH-H	2013	63 \pm 33	23–166	40	67 \pm 31	189 \pm 49	110–269	15	Taylor et al. (2019)
Mt. Desert Island	BH-L	2013	84 \pm 24	55–148	12	106 \pm 37	118 \pm 34	60–217	23	Taylor et al. (2019)
Mt. Desert Island	NEC-H	2013	111 \pm 28	80–137	5	122 \pm 33				Taylor et al. (2019)
Mt. Desert Island	NEC-L	2013	81 \pm 62	21–167	5	83 \pm 64	104 \pm 27	78–149	5	Taylor et al. (2019)
Penobscot River	O	2016	433 \pm 116	304–575	5	475 \pm 117				
Penobscot River	V	2016	338 \pm 112	241–518	5	357 \pm 110				

(continued on next page)

Table 2 (continued)

system	site code	sample year	<i>Fundulus heteroclitus</i>				<i>Menidia menidia</i>			Data Source
			mean ± st. dev. MeHg (ng/g DW)	range MeHg (ng/g DW)	n	mean ± st. dev. MeHg LNST (ng/g DW)	mean ± st. dev. THg (ng/g DW)	range THg (ng/g DW)	n	
Penobscot River										
Webhannet River	DI-H	2015	30 ± 9	18–40	5	30 ± 9	34 ± 4	28–39	5	
Webhannet River	DI-L	2015	19 ± 9	7–31	5	18 ± 9	41 ± 5	38–48	5	
Webhannet River	SM-H	2015	25 ± 7	19–37	5	25 ± 7	45 ± 5	41–54	5	
Webhannet River	SM-L	2015	52 ± 26	13–73	5	52 ± 26	57 ± 16	42–82	5	

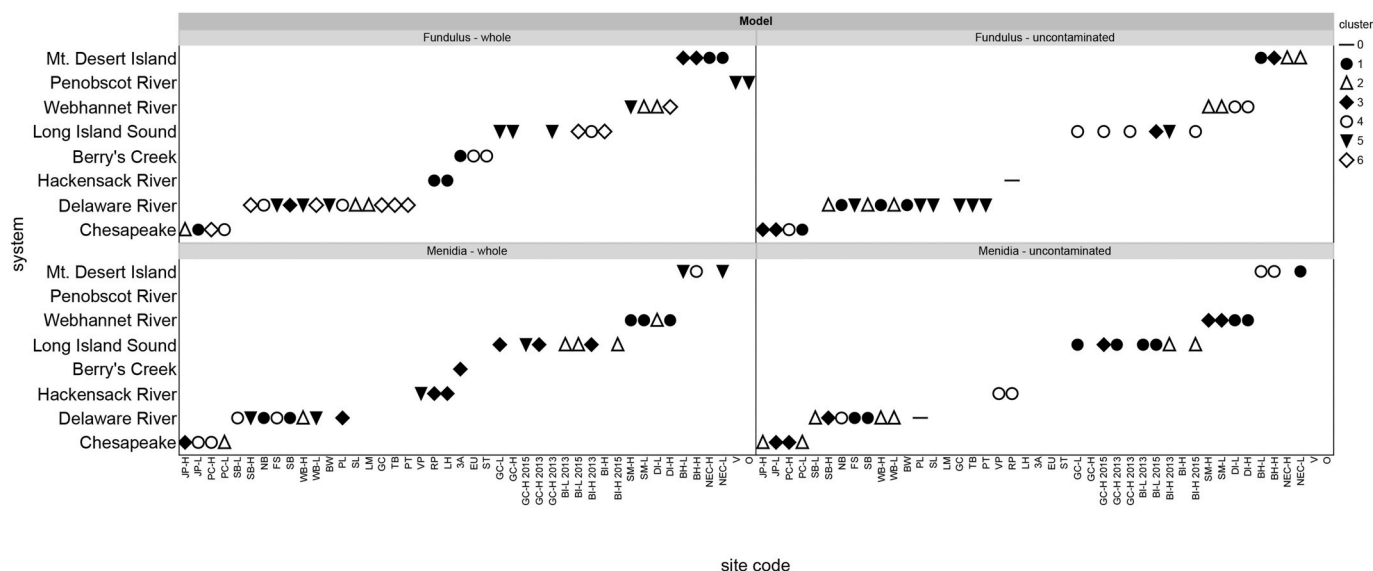


Fig. 2. Model cluster designations for each site and system.

small, local-scale drivers of MeHg production and influences on water column concentrations have greater impact on bioaccumulation and MeHg fate than regional drivers, with geographic proximity less relevant to bioaccumulation than *in situ* biogeochemical processes.

4.1. Abiotic: Biotic Hg relationships

Sediment and water column concentrations are strongly correlated with tissue concentrations, both across species and across all systems. Broadly, this analysis supports previous research that water column concentrations are strongly predictive of forage fish concentrations in most environments and supports Seelen et al.'s (In Press) conclusion that sediments are an important source of MeHg to the water column only at the most contaminated sites. Bioaccumulation of MeHg into fish is both directly influenced by environmental MeHg concentrations and indirectly influenced by watershed characteristics and water biogeochemistry that controls methylation and uptake processes (Eagles-Smith et al., 2016b). Comparison of within species full and reduced models (particularly for *Fundulus*) demonstrates the influence of highly contaminated sediments on driving these relationships. Over half of the *Fundulus* whole model clusters have strong correlations between fish and sediment MeHg, with all of these clusters containing sites of known contamination. *Menidia* Cluster 3 from the whole model, indicating the strongest relationship with sediment (Figs. 5A and 6A), contains sites from Berry's Creek and the Hackensack River, with known Hg contamination originating from a Superfund site upstream in Berry's

Creek. This again emphasizes the greater influence of sediment concentrations on mercury bioaccumulation and fate at contaminated sites than relatively unimpacted areas. Cluster 3 is also the only cluster to exhibit strong relationships with land use, which we again attribute to the presence of relatively contaminated sites within this cluster contributing to the indirect influence of land use on bioaccumulation. When contaminated sites were removed, fewer clusters indicated strong correlations between sediment and tissue concentrations for both species and the relationship to sediment MeHg was weak when present for most *Menidia* clusters. Chen et al. (2014) did not observe the influence of sediments on both *Fundulus* and *Menidia* tissue concentrations. However, this study included only 1 contaminated site of the 10 studied. The influence of this one site may not have been significant enough in the dataset to reveal the impact of contaminated sediments on tissue concentrations.

We hypothesize that the mechanisms driving MeHg concentrations in sediments to the water column (methylation, exchange, and flux/uptake) are functionally different at contaminated sites, or become the dominant source at contaminated locations, leading to differing routes of exposure for resident fauna, with sediment Hg playing a much larger role at contaminated sites than at relatively unimpacted areas where watershed sources and water column processes dominate. This agrees with previous findings indicating dissolved and particulate fractions are better predictors of bioaccumulation in low trophic level fauna, even when only utilizing single time point measurements (Buckman et al., 2019; Chen et al., 2014; Taylor et al., 2019; Wu et al., 2019). Moreover,

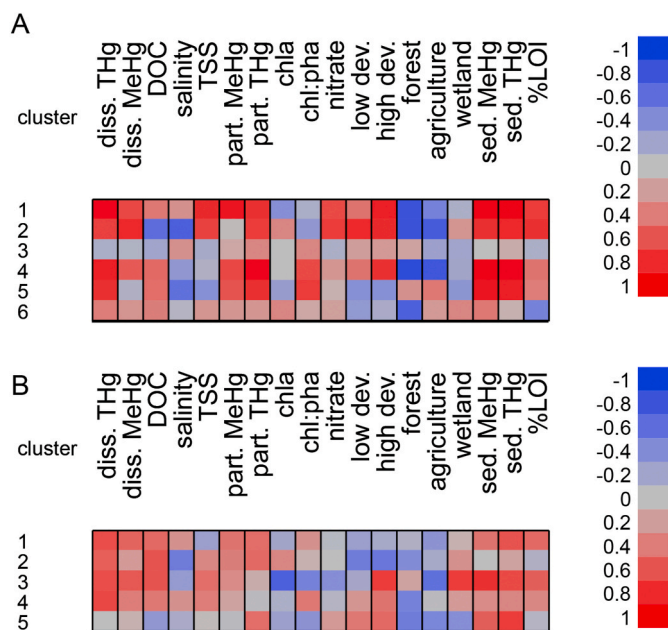


Fig. 3. Heat map by cluster of *Fundulus* tissue MeHg correlations with environmental variables, for all sites combined (A) and for the reduced model with contaminated sites removed (B). Red indicates a positive correlation, blue indicates a negative correlation, and darker colors are a stronger relationship. For example, cluster 1 fish tissues are strongly positively correlated with dissolved Hg, TSS, particulate Hg, high development, and all sed variables, but strongly negatively correlated with % forest in the sub-watershed in panel A. Note that different fish and sites compose the clusters in the different models, so that cluster 1 in panel A does not represent the same sites as cluster 1 in panel B (see Fig. 2). (For interpretation of the references to color in this figure legend, the reader is referred to the Web version of this article.)

dissolved MeHg, dissolved THg, and particulate MeHg all display similar relationships with forage fish Hg concentrations (with the exception of clusters containing Mt. Desert Island sites); indicating that general water column MeHg is strongly influential on bioaccumulation in these species. Sediment concentrations can be particularly confounding when sediment is not a source of MeHg to the water column, but rather a sink, as occurs in some systems (Balcom et al., 2015; Li et al., 2016). Additionally, bulk sediment measurements are not well correlated with sediment-water flux of MeHg. Resuspended sediment MeHg concentrations are different from that of bulk sediment (Seelen et al., 2018) and dissolved flux of MeHg is more strongly related to sediment chemistry (organic carbon content and redox status) than bulk sediment MeHg (Buckman et al., 2019; Hollweg et al., 2009). Seelen et al. (In Press) propose that water column concentrations are driven by separate processes in contaminated versus unimpacted sites, with recycling of legacy Hg between sediment and water compartments prevalent at contaminated sites and *in situ* watershed processes dominant at uncontaminated sites. Though inclusive of fewer sites, the current analysis supports this hypothesis, indicating that water column concentrations are influential over the broadest number of sites and systems, but that sediment concentrations drive water column concentrations when contaminated sites are included. Due to these differing exposure pathways, contaminated and uncontaminated sites should be considered separately when examining processes driving Hg fate, though the influence of contaminated sites on downstream environments cannot be ignored.

4.2. Species-specific factors influencing tissue concentrations

In past studies, as well as in this data set, we have generally observed greater variation and larger ranges in abiotic total and MeHg concentrations than in biota (e.g. (Chen et al., 2014; Chen et al., 2009)), which

would indicate that bioaccumulation is not driven solely by exposure concentration but is strongly mediated by ecological, biogeochemical, and environmental factors (Eagles-Smith et al., 2018). Overall, *Fundulus* show strong relationships to both sediment and water column THg and MeHg concentrations, indicating that these forage fish are important vectors for benthic-pelagic coupling and mercury transfer in estuarine systems due to their feeding ecology. The relationship with sediment is stronger at contaminated sites, but sediment concentration also appeared to be an important driver of bioaccumulation under certain conditions at less impacted sites. In a recent study of coastal lagoons, the relationship of sediment and water column Hg to *Fundulus* and *Menidia*, respectively, was very distinct reflecting their different feeding strategies (Chen et al., 2021). *Fundulus* are omnivorous, and typically feed near the bottom of the estuary, often on salt marshes during high tides. While they will eat detritus when prey are scarce, preferential foraging is on small crustaceans and there is evidence that their food sources can be based on benthic microalgae, rather than pelagic phytoplankton. They feed on locally produced rather than allochthonous contributions (Allen et al., 1994; Currin et al., 2003; James-Pirri et al., 2001; McMahan et al., 2005; Valiela et al., 1977). *Menidia*, in contrast, forage more pelagically with lesser benthic influence, their diet consisting of small zooplankton (mostly crustaceans), plant material and at times, insects (Cadigan and Fell, 1985; Fry et al., 2008; Griffin and Valiela, 2001). These differences in feeding mode and dietary pathways are reflected by the differing influence of sediment Hg on tissue concentrations. Additionally, *Fundulus* exhibit relatively strong site fidelity (McMahon et al., 2005), whereas *Menidia* are transient, wintering offshore with estuarine populations dominated by young-of-the-year and juveniles (Conover and Murawski, 1982), impacting transport of benthic- or pelagic-sourced MeHg through the trophic relay. The ecological characteristics of each species are critical components for understanding the differing exposure routes and resultant within cluster correlations with abiotic variables and explain the consistently stronger sediment influence for *Fundulus* than *Menidia*, even at uncontaminated sites.

4.3. Within cluster patterns and potential drivers of bioaccumulation

Despite the broad patterns of abiotic Hg concentrations being most related to tissue concentrations, and sediments being more important Hg sources to fish in areas of known Hg contamination, there are still differences within each species-specific analysis and observable variation in relationships between fish tissue concentrations and environmental variables across clusters. The pattern of geographically disparate sites within the same cluster indicates the greater importance of small scale local factors on driving bioaccumulation rather than watershed scale, system-wide, or regional relationships. The clusters enable us to see that bioaccumulation at some sites is driven by sediment concentrations, whereas others are more influenced by water column dynamics, with both contamination and ecology influencing the degree and importance of abiotic Hg variables and indirect landscape influences. Strong relationships with land use were only observed when all sites were included in the model (positive with development and negative with forest and agriculture) which is likely an indirect indicator of Hg loading at contaminated sites (which are generally more urban in this data set) rather than forests directly mediating uptake into the food web. This contrast with lakes and streams which show negative relationships between fish Hg and development (Chalmers et al., 2014; Chen et al., 2005). While we were not able to assign one overarching suite of variables that would allow for prediction of bioaccumulation across all Northeast US estuarine sites, we were able to see that contaminated sites behave differently than uncontaminated locations and that small scale processes are particularly important at uncontaminated sites where non-Hg components become more influential. The importance of local scale processes on driving bioaccumulation has also been observed in the San Francisco Bay estuary (Willacker et al., 2017). For the majority of unimpacted sites and systems, local water column concentrations

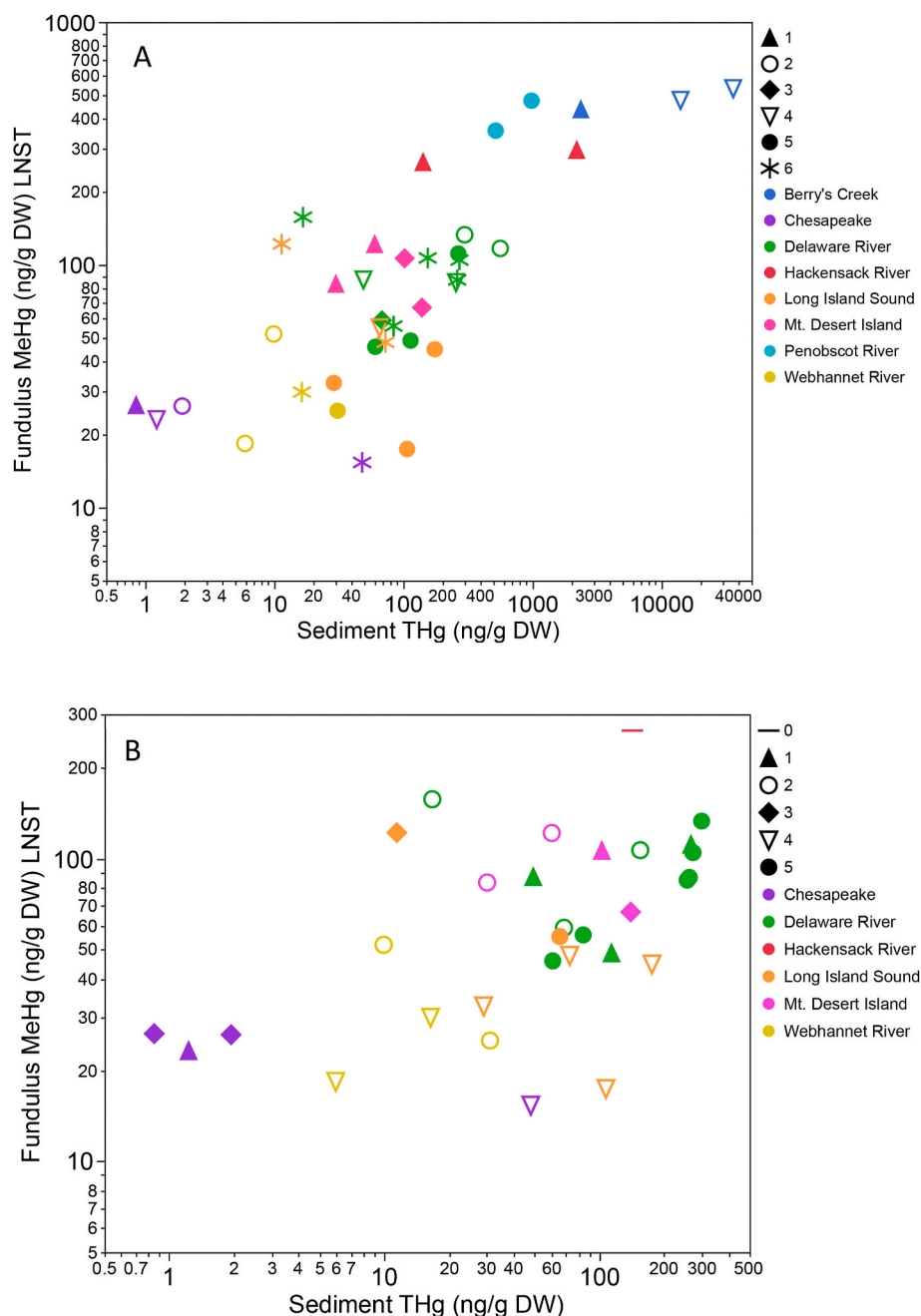


Fig. 4. Fundulus mean length standardized tissue concentration in relation to sediment THg. A) whole model with all sites. The system the fish came from is indicated by the color of the symbol and the cluster assignment is indicated by symbol shape. Known contaminated sites all have sediment concentrations above 400 ng/g DW. For all sites combined there is a positive relationship between sediment THg and Fundulus MeHg ($R^2=0.52$, $p<0.0001$) but this is stronger within some individual clusters. B) model without contaminated sites indicating reduced influence of sediment on tissue concentrations for most clusters.

(even single time point MeHg measurements) may be most useful for predicting bioaccumulation into low trophic level forage fish. Examination of within cluster patterns allows us to hypothesize when and where particular processes may dominate.

Of particular interest is when/where sediment remains a driver of bioaccumulation at uncontaminated sites. For example, *Fundulus* uncontaminated cluster 3 indicates a strong relationship between tissues and sediment MeHg (Figs. 3B and 4B). This cluster contains two sites from the Chesapeake, one site from Long Island, and one site from Mt. Desert Island (Fig. 2), so system-wide Hg loading is likely not driving sediment tissue relationships. Instead, this cluster may be characterized by high flux rates from sediments to the overlying water as there is evidence of correlations between sediment and dissolved concentrations for these sites. Three of the four sites in this cluster are characterized by relatively sandy, low %LOI sediments, which would facilitate sediment water exchange. The fourth site, Bass Harbor, has higher sediment

carbon content, but relatively high levels of upstream Hg and MeHg inputs and sediments here have been shown to be a sink, rather than a source of MeHg, at least for part of the year (Balcom et al., 2015). The upstream inputs and high water column concentrations may drive the strong relationship between fish and dissolved MeHg at this site in addition to the sediment contribution to the water column from the other sites in the cluster. Additionally, this cluster suggests strong relationships ($r>0.6$) between dissolved Hg and MeHg and DOC, sediment Hg and MeHg, and wetlands. While no definitive conclusions can be drawn with only four sites, it does suggest that sites within this cluster may be influenced by greater sediment water exchange than other non-contaminated sites.

In contrast, *Fundulus* uncontaminated cluster 5 (7 sites) has a moderate to strong relationship between sediment and tissue (Fig. 5B), but no other noteworthy correlations between site environmental variables, suggesting that the linkage here may be due to feeding patterns as

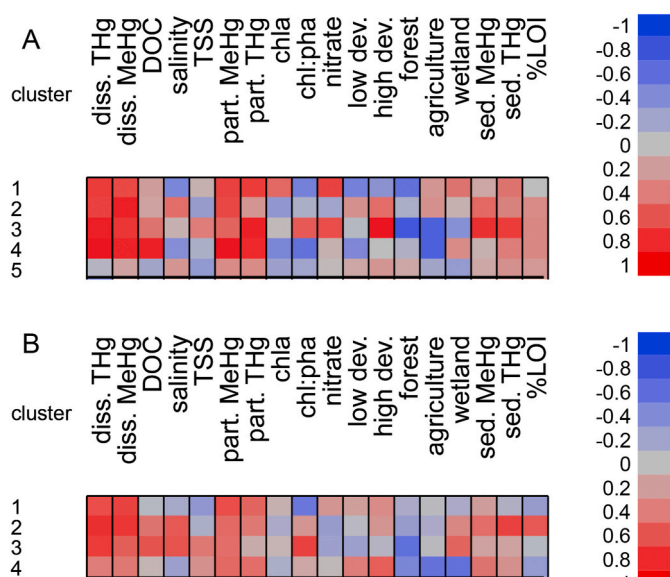


Fig. 5. Heat map of within cluster correlations for *Menidia* THg with environmental variables A) from all sites combined and B) from only uncontaminated sites cluster analysis. Red indicates a positive correlation, blue indicates a negative correlation, and darker colors are a stronger relationship. (For interpretation of the references to color in this figure legend, the reader is referred to the Web version of this article.)

opposed to biogeochemical cycling, with fish eating more detrital material or benthic algae and infauna than in other clusters. Moreover, 5 of the 7 sites are from the Upper Delaware between Philadelphia PA and New Castle DE, an area which is both urbanized and within the estuarine turbidity maximum (ETM). Our previous research indicated that particularly under low flow conditions the sediments are an important source of MeHg to the water column (Gosnell et al., 2016). However ETMs are also associated with sediment and particle trapping through cycles of deposition and resuspension (Sommerfield and Wong, 2011) and may limit primary production through decreased light penetration (Pennock and Sharp, 1986). These factors may contribute to relatively higher sediment Hg loadings and flux, increasing influence of sediment (similar to contaminated sites), detritus, and particle availability to foraging *Fundulus* within the upper Delaware and cluster 5 sites. For *Menidia* from uncontaminated sites, cluster 2 shows a weak to moderate relationship of sediment Hg with tissue THg (Fig. 5B), somewhat surprising given the pelagic feeding mode. We hypothesize that influences on *Menidia* bioaccumulation at these sites are similar to *Fundulus* cluster 5, with relatively higher benthic inputs of locally sourced MeHg (including detrital particles and benthic algae) to the food web driving tissue concentrations rather than elevated external Hg and MeHg loading to the system. However further research is needed to clarify functional and causal linkages between benthic and pelagic sources as well as internal and external MeHg inputs and uptake into the food web.

For other clusters, where sediment is not as influential, watershed sources of Hg may dominate loading and uptake. For example, both species of fish indicated negative associations between fish tissue concentrations and the amount of forested and agricultural land within the sub-watershed. This contrasts with freshwater systems where undisturbed watersheds are typically associated with more efficient methylation and higher fish concentrations (Chalmers et al., 2014; Chan et al., 2012; Chen et al., 2005; Riva-Murray et al., 2020). Overall, freshwater findings, which are mostly focused on locations without local point source contamination, suggest that atmospheric deposition is the greatest source of Hg to those sites, whereas estuaries are repositories of all upstream and local contaminant inputs, including atmospheric deposition of Hg and direct inputs to the upstream watershed and to the estuarine site itself (Kocman et al., 2017). The consistent negative

correlation between fish concentrations and forest cover could be indicative of retention of Hg from terrestrial runoff in freshwaters, thus reducing Hg transport to the estuary in systems with high amounts of forest cover in the sub-watershed (though positive correlations between forest cover and dissolved Hg in some clusters with negative fish:forest relationships would counter this hypothesis). The type and quality of organic carbon loading coming from forested landscapes may also impact availability of inorganic Hg for methylation and MeHg for uptake into phytoplankton relative to less forested watersheds (e.g. Bravo et al., 2017). Similarly, watersheds with higher levels of agricultural land use may be impacted by nutrient runoff, increasing primary production and subsequently biodilution and growth dilution of MeHg within the food web (Driscoll et al., 2012; Gosnell and Mason, 2015; Karimi et al., 2007; Luengen and Russell Flegal, 2009). The weak but mostly negative relationships between chl:a and fish concentrations for uncontaminated sites lends support to this interaction (Figs. 3B and 5B). Moreover, opposing patterns in lotic and lentic systems (Riva-Murray et al., 2020) suggest that observations linking land use and Hg bioaccumulation in freshwater environments may not be directly transferrable to biogeochemically and hydrologically distinct estuarine systems, contributing to the opposite relationships with land use observed here relative to previous freshwater analyses. The current analysis cannot tease out the nuances of these indirect influences (e.g. differences in the relationship with agriculture between watersheds containing crop lands versus pastures can't be determined), but does allow us to observe that these patterns exist on a broad regional scale in Northeast US estuaries. The cluster analysis allows us to make predictions of the major non-sediment loading processes that may be important at uncontaminated sites, but additional measurements are needed to characterize definitive relationships. Regardless, it is apparent that small-scale biogeochemical processes determine water column MeHg concentrations in the systems studied here (Seelen et al., In Press) and these concentrations are most directly relevant to predicting forage fish tissue concentrations.

5. Conclusion

Abiotic exposure concentrations are the most important indicators of bioaccumulation across a broad range of sites for both species of fish, with the importance of land use, primary productivity, and other ancillary variables of secondary importance in determining MeHg concentrations and thus exposure to resident fish. The role of bulk sediment Hg concentration on tissue concentration varies with location and species. *Fundulus*, due to their benthic foraging, are more susceptible to direct exposure to sediment sources of MeHg, and are vectors for transfer of contaminants from sediments to pelagic food webs. This exposure route is most important when there is high Hg loading to the sediments from a point source. Highly contaminated sediments are also important vectors of dietary exposure for the pelagic feeder, *Menidia*, but likely through diffuse flux and particle resuspension as seen with filter feeders (Buckman et al., 2019) rather than through direct ingestion of sediments and benthic algae, detritus, and infauna as for the benthic foragers. It is clear that whether a site has highly contaminated sediments or not must be considered when addressing bioaccumulation of MeHg into lower trophic level fauna. We propose that contaminated sites should be considered separately as they appear to follow separate patterns in determining abiotic concentrations (Seelen et al., In Press) and tissue concentrations. However, as contaminated sites are generally upstream, their impacts may be felt at downstream sites and Hg transport must be considered. For relatively unimpacted sites, the variables driving Hg fate become more varied and nuanced. Most importantly, the analysis has shown that small scale dynamics and environmental variables are dominant over sub-watershed or regional patterns. What drives bioaccumulation at one site may not be the same for a nearby area or at a site with similar sub-watershed land uses. The importance of scale bears further investigation, but exposure through water and sediment remains

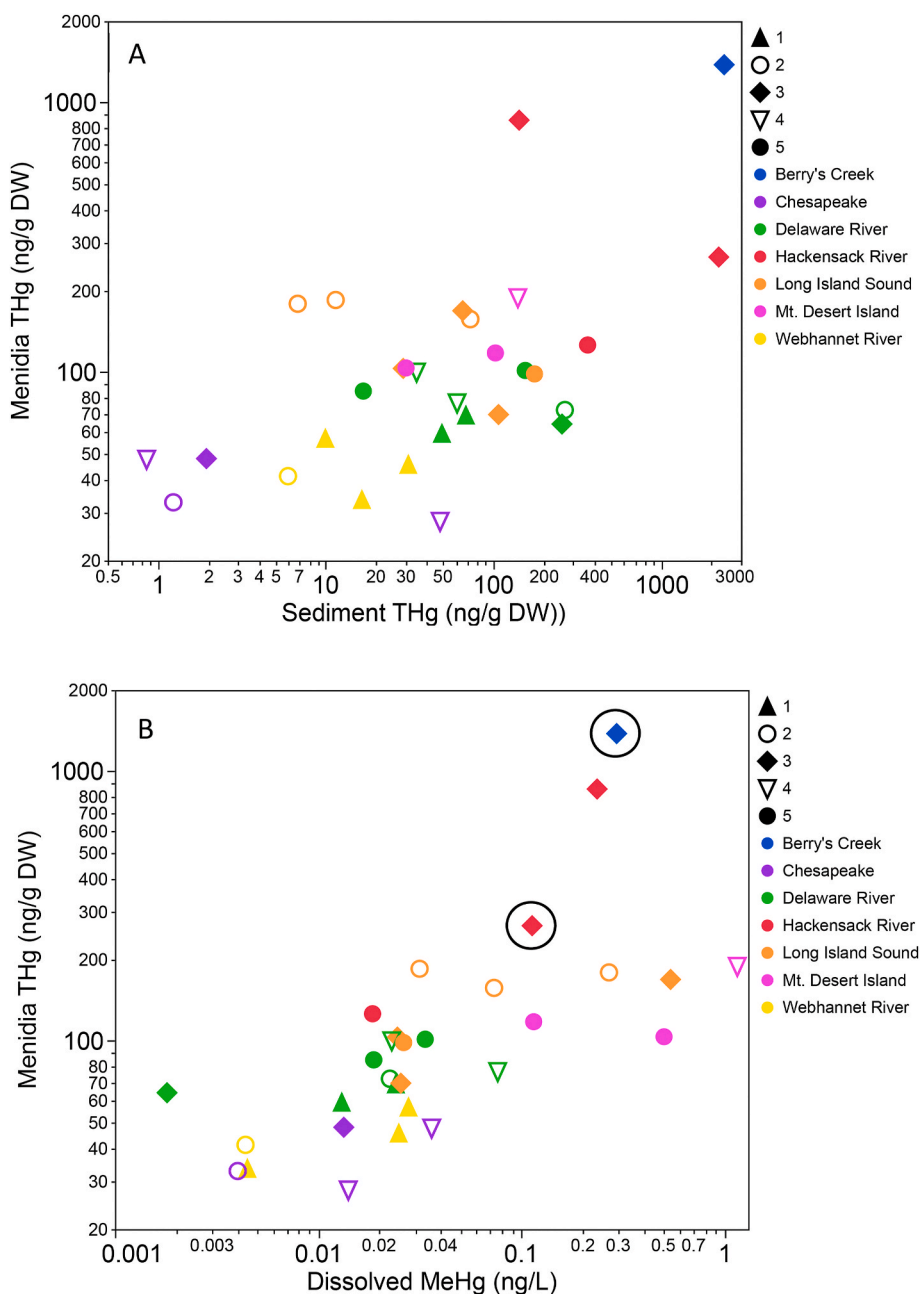


Fig. 6. A) Sediment THg versus mean tissue THg for Menidia by cluster for all sites. The system the fish came from is indicated by the color of the symbol and the cluster assignment is indicated by symbol shape. There is a weak relationship between sediment and tissue for all sites combined ($R^2=0.20$, $p<0.001$) but mixed relationships within clusters. B) Mean Menidia THg plotted against dissolved MeHg, indicating the strong relationship across all sites combined ($R^2=0.43$, $p<0.0001$) as well as within cluster assignments. The two contaminated sites are indicated by a black circle. Removal of these sites changed the cluster assignments (Fig. 2) but not the strong positive relationships with water column MeHg within clusters (Figure S2). (For interpretation of the references to color in this figure legend, the reader is referred to the Web version of this article.)

the most consistent observable influence on fish tissue concentrations.

Credit author statement

Kate Buckman: Investigation, Formal analysis, Data curation, Writing – original draft. Robert Mason: Conceptualization, Investigation, Writing-Review & Revision, Visualization, Supervision, Funding acquisition. Emily Seelen: Investigation, Data curation, Writing-Review & Revision, Visualization. Vivien Taylor: Investigation, Data curation, Writing-Review & Revision. Prentiss Balcom: Investigation, Writing-Review & Revision. Jonathan Chipman: Resources, Writing-Review & Revision, Visualization. Celia Chen: Conceptualization, Investigation, Writing-Review & Revision, Supervision, Funding acquisition

Funding

National Institute of Environmental Health Sciences (Chen P42

ES007373), (Chen, R01 ES021950). USDA Forest Service (Nislow, 09-JV-11242307-124). IACUC approval: Dartmouth protocols chen_cy_1 (approved 2013) and chen_cy_1.2 (approved 2016).

Declaration of competing interest

The authors declare that they have no known competing financial interests or personal relationships that could have appeared to influence the work reported in this paper.

Acknowledgements

We would like to thank H. Roebuck, K. Gosnell, V. Ortiz, A. Schartup, G. Hansen, W. Huffman, N. Mazrui, B. DiMento, and A. Curtis for assistance with field collections and sample analysis. J. Hua provided helpful discussion and guidance regarding machine learning techniques. This work was funded by grants from The National Institute of

Environmental Health Sciences (Chen P42 ES007373), (Chen, R01 ES021950), and the USDA Forest Service (Nislow, 09-JV-11242307-124).

Appendix A. Supplementary data

Supplementary data to this article can be found online at <https://doi.org/10.1016/j.envres.2020.110629>.

References

- Allen, E.A., Fell, P.E., Peck, M.A., Gieg, J.A., Guthke, C.R., Newkirk, M.D., 1994. Gut contents of common mummichogs, *Fundulus heteroclitus* L., in a restored impounded marsh and in natural reference marshes. *Estuaries* 17, 462–471.
- Amos, H.M., Jacob, D.J., Kocman, D., Horowitz, H.M., Zhang, Y.X., Dutkiewicz, S., Horvat, M., Corbitt, E.S., Krabbenhoft, D.P., Sunderland, E.M., 2014. Global biogeochemical implications of mercury discharges from rivers and sediment burial. *Environ. Sci. Technol.* 48, 9514–9522.
- Balcom, P.H., Schartup, A.T., Mason, R.P., Chen, C.Y., 2015. Sources of water column methylmercury across multiple estuaries in the Northeast US. *Mar. Chem.* 177, 721–730.
- Bergamaschi, B.A., Fleck, J.A., Downing, B.D., Boss, E., Pellerin, B.A., Ganju, N.K., Schoellhamer, D.H., Byington, A.A., Heim, W.A., Stephenson, M., Fujii, R., 2012. Mercury dynamics in a San Francisco estuary tidal wetland: assessing dynamics using in situ measurements. *Estuar. Coast* 35, 1036–1048.
- Bravo, A.G., Bouchet, S., Tolu, J., Bjorn, E., Mateos-Rivera, A., Bertilsson, S., 2017. Molecular composition of organic matter controls methylmercury formation in boreal lakes. *Nat. Commun.* 8.
- Bravo, A.G., Kothawala, D.N., Attermeyer, K., Tessier, E., Bodmer, P., Ledesma, J.U., Audet, J., Casas-Ruiz, J.P., Catalan, N., Cauvy-Fraunie, S., Colls, M., Deininger, A., Evtimova, V.V., Fonville, J.A., Fuss, T., Gilbert, P., Ortega, S.H., Liu, L., Mendoza-Lera, C., Monteiro, J., Mor, J.R., Nagler, M., Niedrist, G.H., Nydahl, A.C., Pastor, A., Pegg, J., Roberts, C.G., Pilotto, F., Portela, A.P., Gonzalez-Quijano, C.R., Romero, F., Rulik, M., Amouroux, D., 2018. The interplay between total mercury, methylmercury and dissolved organic matter in fluvial systems: a latitudinal study across Europe. *Water Res.* 144, 172–182.
- Buckman, K., Taylor, V., Broadley, H., Hocking, D., Balcom, P., Mason, R., Nislow, K., Chen, C., 2017. Methylmercury bioaccumulation in an urban estuary: Delaware river, USA. *Estuar. Coast* 40, 1358–1370.
- Buckman, K.L., Seelen, E.A., Mason, R.P., Balcom, P., Taylor, V.F., Ward, J.E., Chen, C.Y., 2019. Sediment organic carbon and temperature effects on methylmercury concentration: a mesocosm experiment. *Sci. Total Environ.* 666, 1316–1326.
- Cadigan, K.M., Fell, P.E., 1985. Reproduction, growth and feeding habits of *Menidia menidia* (Atherinidae) in a tidal marsh-estuarine system in southern New England. *Copeia* 21–26.
- Chalmers, A.T., Krabbenhoft, D.P., Van Metre, P.C., Nilles, M.A., 2014. Effects of urbanization on mercury deposition and New England. *Environ. Pollut.* 192, 104–112.
- Chan, C., Heinbokel, J.F., Myers, J.A., Jacobs, R.R., 2012. A dynamic model using monitoring data and watershed characteristics to project fish tissue mercury concentrations in stream systems. *Integrated Environ. Assess. Manag.* 8, 709–722.
- Chen, C., Amirbahman, A., Fisher, N., Harding, G., Lamborg, C., Nacci, D., Taylor, D., 2008. Methylmercury in marine ecosystems: spatial patterns and processes of production, bioaccumulation, and biomagnification. *EcoHealth* 5, 399–408.
- Chen, C., Buckman, K., Shaw, A., Curtis, A., Taylor, M., Montesdeoca, M.R., Driscoll, C.T., 2021. The influence of nutrient loading on methylmercury availability in Long Island estuaries. *Environ. Pollut.* 268.
- Chen, C.Y., Borsuk, M.E., Bugge, D.M., Hollweg, T., Balcom, P.H., Ward, D.M., Williams, J., Mason, R.P., 2014. Benthic and pelagic pathways of methylmercury bioaccumulation in estuarine food webs of the Northeast United States. *PLoS One* 9.
- Chen, C.Y., Dionne, M., Mayes, B.M., Ward, D.M., Sturup, S., Jackson, B.P., 2009. Mercury bioavailability and bioaccumulation in estuarine food webs in the Gulf of Maine. *Environ. Sci. Technol.* 43, 1804–1810.
- Chen, C.Y., Stemberger, R.S., Kamman, N.C., Mayes, B.M., Folt, C.L., 2005. Patterns of Hg bioaccumulation and transfer in aquatic food webs across multi-lake studies in the northeast US. *Ecotoxicology* 14, 135–147.
- Conover, D.O., Murawski, S.A., 1982. Offshore winter migration of the Atlantic silverside, *Menidia menidia*. *Fish. Bull.* 80, 145–150.
- Curran, C.A., Wainright, S.C., Able, K.W., Weinstein, M.P., Fuller, C.M., 2003. Determination of food web support and trophic position of the mummichog, *Fundulus heteroclitus*, in New Jersey smooth cordgrass (*Spartina alterniflora*), common reed (*Phragmites australis*), and restored salt marshes. *Estuaries* 26, 495–510.
- Driscoll, C.T., Chen, C.Y., Hammerschmidt, C.R., Mason, R.P., Gilmour, C.C., Sunderland, E.M., Greenfield, B.K., Buckman, K.L., Lamborg, C.H., 2012. Nutrient supply and mercury dynamics in marine ecosystems: a conceptual model. *Environ. Res.* 119, 118–131.
- Eagles-Smith, C.A., Ackerman, J.T., 2014. Mercury bioaccumulation in estuarine wetland fishes: evaluating habitats and risk to coastal wildlife. *Environ. Pollut.* 193, 147–155.
- Eagles-Smith, C.A., Ackerman, J.T., Willacker, J.J., Tate, M.T., Lutz, M.A., Fleck, J.A., Stewart, A.R., Wiener, J.G., Evers, D.C., Lepak, J.M., Davis, J.A., Pritz, C.F., 2016a. Spatial and temporal patterns of mercury concentrations in freshwater fish across the Western United States and Canada. *Sci. Total Environ.* 568, 1171–1184.
- Eagles-Smith, C.A., Silbergeld, E.K., Basu, N., Bustamante, P., Diaz-Barriga, F., Hopkins, W.A., Kidd, K.A., Nyland, J.F., 2018. Modulators of mercury risk to wildlife and humans in the context of rapid global change. *Ambio* 47, 170–197.
- Eagles-Smith, C.A., Wiener, J.G., Eckley, C.S., Willacker, J.J., Evers, D.C., Marvin-DiPasquale, M., Obrist, D., Fleck, J.A., Aiken, G.R., Lepak, J.M., Jackson, A.K., Webster, J.P., Stewart, A.R., Davis, J.A., Alpers, C.N., Ackerman, J.T., 2016b. Mercury in western North America: a synthesis of environmental contamination, fluxes, bioaccumulation, and risk to fish and wildlife. *Sci. Total Environ.* 568, 1213–1226.
- Evers, D.C., Mason, R.P., Kamman, N.C., Chen, C.Y., Bogomolni, A.L., Taylor, D.L., Hammerschmidt, C.R., Jones, S.H., Burgess, N.M., Munney, K., Parsons, K.C., 2008. Integrated mercury monitoring program for temperate estuarine and marine ecosystems on the North American Atlantic coast. *EcoHealth* 5, 426–441.
- Fry, B., Cieri, M., Hughes, J., Tobias, C., Deegan, L.A., Peterson, B., 2008. Stable isotope monitoring of benthic-planktonic coupling using salt marsh fish. *Mar. Ecol. Prog. Ser.* 369, 193–204.
- Gosnell, K., Balcom, P., Ortiz, V., DiMento, B., Schartup, A., Greene, R., Mason, R., 2016. Seasonal cycling and transport of mercury and methylmercury in the turbidity maximum of the Delaware estuary. *Aquat. Geochem.* 22, 313–336.
- Gosnell, K.J., Mason, R.P., 2015. Mercury and methylmercury incidence and bioaccumulation in plankton from the central Pacific Ocean. *Mar. Chem.* 177, 772–780.
- Griffin, M.P.A., Valiela, I., 2001. Delta N-15 isotope studies of life history and trophic position of *Fundulus heteroclitus* and *Menidia menidia*. *Mar. Ecol. Prog. Ser.* 214, 299–305.
- Hammerschmidt, C.R., Fitzgerald, W.F., 2001. Formation of artifact methylmercury during extraction from a sediment reference material. *Anal. Chem.* 73, 5930–5936.
- Hammerschmidt, C.R., Fitzgerald, W.F., 2006. Methylmercury cycling in sediments on the continental shelf of southern New England. *Geochem. Cosmochim. Acta* 70, 918–930.
- Hayer, C.A., Chipps, S.R., Stone, J.J., 2011. Influence of physiochemical and watershed characteristics on mercury concentration in walleye, *Sander vitreus*. *M. Bull. Environ. Contam. Toxicol.* 86, 163–167.
- Hollweg, T.A., Gilmour, C.C., Mason, R.P., 2009. Methylmercury production in sediments of Chesapeake Bay and the mid-Atlantic continental margin. *Mar. Chem.* 114, 86–101.
- Homer, C., Dewitz, J., Yang, L.M., Jin, S., Danielson, P., Xian, G., Coulston, J., Herold, N., Wickham, J., Megown, K., 2015. Completion of the 2011 national land cover database for the conterminous United States - representing a decade of land cover change information. *Photogramm. Eng. Rem. Sens.* 81, 345–354.
- Horvat, M., Bloom, N.S., Liang, L., 1993. Comparison of distillation with other current isolation methods for the determination of methyl mercury compound in low-level environmental samples 1. Sediments. *Anal. Chim. Acta* 281, 135–152.
- James-Pirri, M.J., Raposa, K.B., Catena, J.G., 2001. Diet composition of mummichogs, *Fundulus heteroclitus*, from restoring and unrestricted regions of a New England (USA) salt marsh. *Estuar. Coast Shelf Sci.* 53, 205–213.
- Kamman, N.C., Chalmers, A., Clair, T.A., Major, A., Moore, R.B., Norton, S.A., Shanley, J.B., 2005. Factors influencing mercury in freshwater surface sediments of northeastern North America. *Ecotoxicology* 14, 101–111.
- Karimi, R., Chen, C.Y., Pickhardt, P.C., Fisher, N.S., Folt, C.L., 2007. Stoichiometric controls of mercury dilution by growth. *Proc. Natl. Acad. Sci. Unit. States Am.* 104, 7477–7482.
- Kneib, R.T., 2000. Salt Marsh Ecosystems and Production Transfers by Estuarine Nekton in the Southeastern United States. Springer, Dordrecht.
- Kocman, D., Wilson, S.J., Amos, H.M., Telmer, K.H., Steenhuisen, F., Sunderland, E.M., Mason, R.P., Outridge, P., Horvat, M., 2017. Toward an assessment of the global inventory of present-day mercury releases to freshwater environments. *Int. J. Environ. Res. Publ. Health* 14.
- Kramer, D., Goodale, W.M., Kennedy, L.M., Carstensen, L.W., Kaur, T., 2005. Relating land cover characteristics and common loon mercury levels using geographic information systems. *Ecotoxicology* 14, 253–262.
- Lavoie, R.A., Amyot, M., Lapierre, J.F., 2019. Global meta-analysis on the relationship between mercury and dissolved organic carbon in freshwater environments. *J. Geophys. Res.-Biogeosci.* 124, 1508–1523.
- Lavoie, R.A., Jardine, T.D., Chumchal, M.M., Kidd, K.A., Campbell, L.M., 2013. Biomagnification of mercury in aquatic food webs: a worldwide meta-analysis. *Environ. Sci. Technol.* 47, 13385–13394.
- Li, M.L., Schartup, A.T., Valberg, A.P., Ewald, J.D., Krabbenhoft, D.P., Yin, R.S., Bolcom, P.H., Sunderland, E.M., 2016. Environmental origins of methylmercury accumulated in subarctic estuarine fish indicated by mercury stable isotopes. *Environ. Sci. Technol.* 50, 11559–11568.
- Luengen, A.C., Russell Flegal, A., 2009. Role of phytoplankton in mercury cycling in the San Francisco Bay estuary. *Limnol. Oceanogr.* 54, 23–40.
- McMahon, K.W., Johnson, B.J., Ambrose, W.G., 2005. Diet and movement of the killifish, *Fundulus heteroclitus*, in a Maine salt marsh assessed using gut contents and stable isotope analyses. *Estuaries* 28, 966–973.
- Mitchell, C.P.J., Gilmour, C.C., 2008. Methylmercury production in a Chesapeake Bay salt marsh. *J. Geophys. Res.-Biogeosci.* 113.
- Mitchell, C.P.J., Jordan, T.E., Heyes, A., Gilmour, C.C., 2012. Tidal exchange of total mercury and methylmercury between a salt marsh and a Chesapeake Bay sub-estuary. *Biogeochemistry* 111, 583–600.
- Munson, K.M., Babi, D., Lamborg, C.H., 2014. Determination of monomethylmercury from seawater with ascorbic acid-assisted direct ethylation. *Limnol. Oceanogr. Methods* 12, 1–9.
- Pennock, J.R., Sharp, J.H., 1986. Phytoplankton production in the Delaware Estuary: temporal and spatial variability. *Mar. Ecol. Prog. Ser.* 34, 143–155.

- Riva-Murray, K., Richter, W., Razavi, N.R., Burns, D.A., Cleckner, L.B., Burton, M., George, S.D., Freehafer, D., 2020. Mercury in fish from streams and rivers in New York State: spatial patterns, temporal changes, and environmental drivers. *Ecotoxicology* (29), 1686–1708.
- Riva-Murray, K., Richter, W., Razavi, N.R., Burns, D.A., Cleckner, L.B., Burton, M., George, S.D., Freehafer, D., 2020. Mercury in Fish from Streams and Rivers in New York State: Spatial Patterns, Temporal Changes, and Environmental Drivers. *Ecotoxicology*, London, England).
- Schartup, A.T., Balcom, P.H., Mason, R.P., 2014. Sediment-porewater partitioning, total sulfur, and methylmercury production in estuaries. *Environ. Sci. Technol.* 48, 954–960.
- Schartup, A.T., Mason, R.P., Balcom, P.H., Hollweg, T.A., Chen, C.Y., 2013. Methylmercury production in estuarine sediments: role of organic matter. *Environ. Sci. Technol.* 47, 695–700.
- Seelen, E.A., Chen, C., Balcom, P., Buckman, K., Taylor, V., Mason, R., In Press. Historic contamination alters mercury sources and cycling in temperate estuaries relative to uncontaminated sites. *Water Res.*
- Seelen, E.A., Massey, G.M., Mason, R.P., 2018. Role of sediment resuspension on estuarine suspended particulate mercury dynamics. *Environ. Sci. Technol.* 52, 7736–7744.
- Shi, X.M., Mason, R.P., Charette, M.A., Mazrui, N.M., Cai, P.H., 2018. Mercury flux from salt marsh sediments: insights from a comparison between Ra-224/Th-228 disequilibrium and core incubation methods. *Geochem. Cosmochim. Acta* 222, 569–583.
- Sommerfield, C.K., Wong, K.C., 2011. Mechanisms of sediment flux and turbidity maintenance in the Delaware Estuary. *J. Geophys. Res.: Oceans* 116.
- Sunderland, E.M., 2007. Mercury exposure from domestic and imported estuarine and marine fish in the US seafood market. *Environ. Health Perspect.* 115, 235–242.
- Taylor, V.F., Buckman, K.L., Seelen, E.A., Mazrui, N.M., Balcom, P.H., Mason, R.P., Chen, C.Y., 2019. Organic carbon content drives methylmercury levels in the water column and in estuarine food webs across latitudes in the Northeast United States. *Environ. Pollut.* 246, 639–649.
- Turner, R.R., Mitchell, C.P.J., Kopec, A.D., Bodaly, R.A., 2018. Tidal fluxes of mercury and methylmercury for mendall marsh, Penobscot River estuary, Maine. *Sci. Total Environ.* 637, 145–154.
- Valiela, I., Wright, J.E., Teal, J.M., Volkmann, S.B., 1977. Growth, production and energy transformation in salt marsh killifish *Fundulus heteroclitus*. *Mar. Biol.* 40, 135–144.
- Willacker, J.J., Eagles-Smith, C.A., Ackerman, J.T., 2017. Mercury bioaccumulation in estuarine fishes: novel insights from sulfur stable isotopes. *Environ. Sci. Technol.* 51, 2131–2139.
- Wu, P.P., Kainz, M.J., Bravo, A.G., Akerblom, S., Sonesten, L., Bishop, K., 2019. The importance of bioconcentration into the pelagic food web base for methylmercury biomagnification: a meta-analysis. *Sci. Total Environ.* 646, 357–367.